Apex-enhanced second-harmonic generation by using double-hole arrays in a gold film

A. Lesuffleur, L. K. S. Kumar, and R. Gordon
Department of Electrical and Computer Engineering, University of Victoria, 3800 Finnerty Road, Victoria, BC, V8P5C2, Canada
(Received 25 August 2006; revised manuscript received 25 October 2006; published 18 January 2007)

The enhancement of second harmonic generation (SHG) from arrays of subwavelength double holes in a gold film is studied. Each overlapping double hole, which is created in a straightforward manner by approaching two individual holes, has apexes that are responsible for nanoscale focusing of the electric field. A 14 times enhancement of SHG is measured when compared to the circular hole shape. The angular dependence of the SHG is explained by momentum matching and by symmetry breaking required for SHG. By varying the periodicity of the arrays, the Bragg resonances are tuned and modify the SHG signal. The SHG is shown to be enhanced by a resonance at the second harmonic wavelength. The local enhancement of the electric field presented in this work shows that the double-hole structure is a good candidate for applications such as surface-enhanced Raman spectroscopy and nonlinear optics.

DOI: 10.1103/PhysRevB.75.045423 PACS number(s): 78.66.Bz, 42.65.Ky, 42.25.Fx, 73.20.Mf

I. INTRODUCTION

A primary objective of nanophotonics is to increase and localize the light intensity to subwavelength regions. This is important for nonlinear optical processes such as second harmonic generation (SHG),[1] surface-enhanced Raman scattering (SERS) (Ref. 2) and super continuum generation (SCG).[3] It is well known that increased local field intensities can be achieved by using metal nanostructures.[4–7]

In 1998, Ebbesen and co-workers showed that an array of nanoholes in a metallic film enhanced the optical transmission compared to the prediction of the Bethe's theory.[8] More recently, it has been demonstrated that the hole-shape determines the optical properties of arrays of subwavelength holes and of isolated holes in metals.[9,10] The aspect ratio of elliptical and rectangular holes changes the polarization, the transmission intensity, and the cutoff wavelength, both in arrays[11] and in isolated holes.[12,13] The orientation of arrays of elliptical and double holes showed the separate basis and lattice contributions to the transmission.[14] Hole-shapes that enhance the local field intensity are of interest for nonlinear optical interactions with materials, such as second harmonic generation (SHG).

The efficiency of SHG is proportional to the square of the local field intensity. Furthermore, SHG is restricted in centrosymmetric materials such as bulk gold, but it may be observed at the surface where the symmetry is broken. It has been shown experimentally and theoretically that the enhanced local field from rough surface and metallic nanostructures enhances the SHG signal.[15] Individual surface defects on a metallic surface,[16] or nanoscopic metal tips[17] have been studied using SHG. SHG enhancement has been measured for randomly distributed small holes,[18] periodic nanohole arrays in a metallic film,[19] and periodically nanostructured metal film consisting of a single subwavelength aperture surrounded by concentric circular grooves.[20] The SHG from arrays of single holes has been shown to depend on the angle of incidence.[19] For normal incidence, where the array was centrosymmetric, negligible SHG signal was observed as expected.[19]

In this paper, we study the double-hole structure which has an order of magnitude larger SHG signal due to the field localization. This structure consists of two holes which are overlapping to produce two apexes. These two apexes are responsible for the extreme subwavelength focusing of this structure. These double-hole structures are created in a straightforward manner by varying the distance between two individual holes until sharp apexes are formed. Recently, enhanced SHG from the double-hole structure, as compared to the circular and the oblate hole structures, has been presented.[21] In that work, we studied only the center-to-center hole separation for a fixed angle of incidence, where it was shown that the SHG is maximized when the holes are just overlapping to produce two sharp apexes. In this work, we present a comprehensive study of the linear and nonlinear properties of the double-hole structure in a gold film, including the first presentation of the effects of the angle of incidence, array periodicity, with both linear and nonlinear measurements. The angle of incidence is shown to be an important parameter for the SHG, which influences both the momentum matching and symmetry-breaking of the arrays of holes in the gold film. It is shown that two effects lead to enhanced-SHG when changing the array periodicity; the array periodicity has maxima when momentum matching either to the fundamental wavelength or second-harmonic wavelength.

In Sec. II, the experimental techniques for fabrication, linear optical measurements, and nonlinear optical measurements are presented. In Sec. III, the linear and SHG measurements are presented for variations in the center-to-center hole spacing and for variations in the array periodicity. In Sec. IV, the results are further explained to show how the SHG is increased.

II. EXPERIMENTAL TECHNIQUES

A. Fabrication of nanohole arrays

Figure 1 shows a scanning electron microscope image of an array of double-holes milled by a focused ion beam through a 100 nm thick gold layer with a 5 nm Cr adhesion layer on a glass substrate. The gallium ion beam was set to 30 keV for milling with a current of 100 pA. The typical beam spot size was 10 nm. The dwell time of the beam at 1 pixel was 3 ms and the average time taken to mill one array of several thousands of holes was 2 minutes. Each array cov-

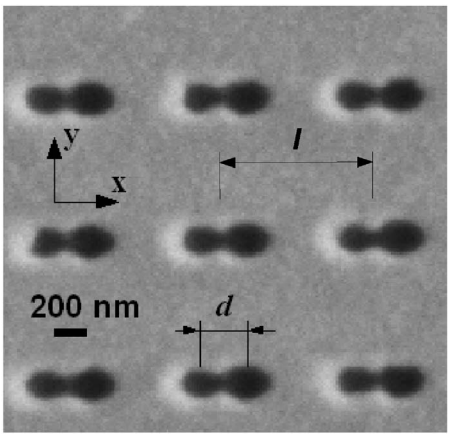

FIG. 1. Scanning electron microscope image for a double-hole array with a spacing of $d=195$ nm and a periodicity $l=750$ nm. x and y polarizations are shown with arrows.

ers a 25×30 μm^2 area. We fabricated two series of arrays. The first series varied only the spacing between the two holes, d, with constant periodicity. The second series used a fixed spacing between the two holes but with varying the periodicity, l, from 380 nm to 750 nm.

B. Linear measurements in transmission

The linear optical transmission measurements were taken with a microscope setup using a 50× microscope objective. The transmission of white light trough the array was collected using a 400 μm core broad-area fiber placed 3 cm away from the sample. The spectra were acquired using an optical spectrum analyzer which operates between 400 nm and 900 nm. A polarizer was placed before the collection fiber to obtain the y polarization as defined with respect to the basis and array, as shown in Fig. 1. The x polarization had over an order of magnitude lower transmission signal.

C. SHG measurements

SHG measurements were performed by using a Ti:Sapphire laser with 30 fs pulses and a center wavelength of 800 nm. The average power incident on the sample was limited to 20 mW. A 20× microscope objective focused the pulse onto the array. The transmitted signal was collimated by a 20× microscope objective, with a large enough working distance to allow for rotation of the sample. The sample was rotated along the x axis from 0° to 15° with a precision of 2°. The polarization of the incident beam was circular, but separate measurements were made for linear polarized incident beams, as indicated. In addition, the polarization of the SHG signal linear was also determined in separate measurements, as indicated in the text. Two blue-green filters (BG40) were used to reduce the fundamental beam by 10^{14}, at the expense of 40% of the SHG signal. The SHG was collected collinear to the incident beam, however, the sample was rotated along the x axis to break the centrosymmetry of the system. The SHG was measured by a streak camera operating in synchroscan photon counting mode. As expected, SHG was only observed when the Ti:Sapphire laser was in pulsed operation,

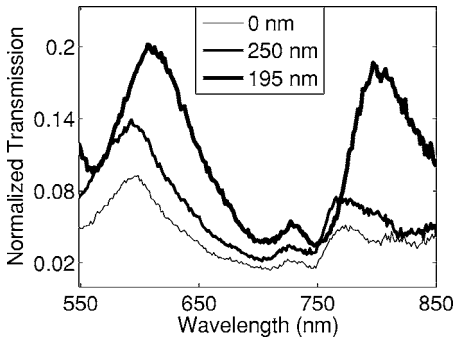

FIG. 2. Linear transmission spectra for different hole spacings, d, (0, 195, and 250 nm). The measurements are normalized to the spectrum of the incident beam.

due to the requirement for high peak power. Furthermore, the pump-power dependence of the SHG signal gave a 2.1 ± 0.1 slope on a log-log plot; almost exactly the expected value of 2 from SHG.

III. RESULTS

A. Center-to-center hole spacing dependence of SHG

Figure 2 shows the linear transmission measurements for three different center-to-center hole spacings, $d=0$ nm, 195 nm, and 250 nm. The periodicity of the arrays is fixed to 750 nm. There are two maxima in transmission around the wavelengths of 600 nm and 800 nm which correspond to the (1,1) and the (1,0) resonances of the gold-air interface. Due to the wavelength of the Ti: Sapphire laser being centered at 800 nm, we focused our attention on the (1,0) resonance.

According to the finite-difference time-domain (FDTD) calculations[22] and to previous measurements,[21] only the y polarization allows the enhancement of the transmission and of the electric field for the (1,0) resonance. The x polarization produces negligible signal, both in the linear transmission and in the SHG measurements. The maximum SHG is seen for linear polarized incident beam along the y direction, as reported previously.[21] As shown with FDTD calculations in Fig. 3, the y polarization gives the strong field enhancement for both the fundamental and second harmonic wavelengths, whereas the x polarization gives no enhancement. This is different from dipolelike systems, such as the optical antenna,[7] bowtie antenna,[6] and double dots,[23] where the x polarization gives the maximum enhancement In the following discussion, only the y polarization is considered. For y polarization incident beam, the y polarized SHG was 12.1 times larger than the x polarized SHG signal. For the x polarization of incidence, the total SHG is reduced by a factor of 49.7.

Figure 4 shows the angular dependent SHG measurements versus the center-to-center hole spacing. The general trend of this figure is that when the holes are nearly overlapping with sharp apexs, they produce the greatest SHG. The SHG was maximized for an angle of 8°.

For angles smaller than 5°, the SHG was weak. For such small angles, the centrosymmetry of the sample is not broken sufficiently; however broken centrosymmetry is necessary to

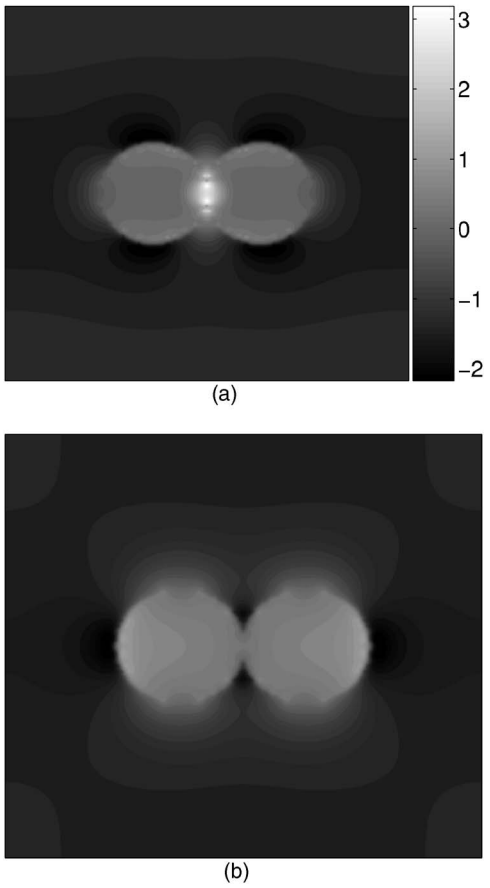

FIG. 3. FDTD calculation of natural logarithm of electric field from double-hole structure with apexes for a 750 nm periodicity with an incident beam polarized along (a) the y direction and (b) the x direction. The colormap is the same for both figures.

measure a SHG signal. A previous work reported that a minimum of 10° was necessary angle to measure any significant signal from an array of circular and triangular holes in a gold film.[19] For the double-hole structure of this work, by tilting the sample past 5°, the SHG increased significantly. This was mainly the case for the two nearly-overlapping hole arrays with sharp apexes, with center-to-center hole spacing of 190 nm and 195 nm. For all the other arrays, the SHG signal remained weak below a 10° angle of incidence. For the 8° angle of incidence, there was a significant enhancement of SHG for the array with a 195 nm center-to-center distance between the two holes, whereas the 190 nm array showed maximum SHG for other angles.

For angles larger than 12°, the SHG decreased. This may be the result because there was no longer good momentum matching between the transmission resonance and the fundamental wavelength. The linear transmission of the fundamental wavelength also decreased (not shown in the figures) as the angle of incidence was increased, which supports this hypothesis. The maximum of SHG for each array arises for different angles of incidence; the larger the center-to-center distance, the smaller the maximum SHG angle of incidence. This phenomenon will be discussed further in the Sec. IV.

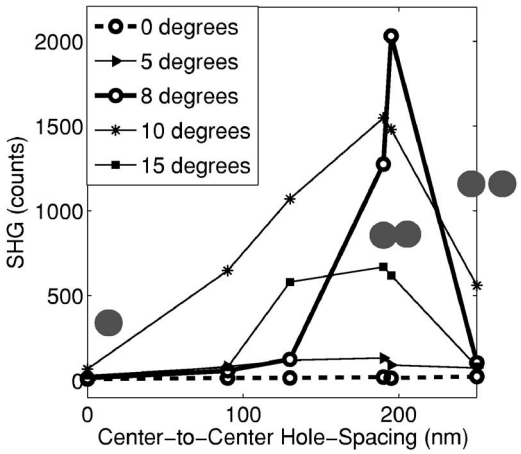

FIG. 4. Angle-dependent SHG measurements as a function of center-to-center hole spacing. $d=0$ nm corresponds to a circular shape while the $d=250$ nm consists in two holes separated by a gap of 50 nm. The array periodicity was 750 nm.

B. Periodicity dependence of SHG

A second set of samples was fabricated with varying lattice periodicity, l, and fixed center-to-center hole-spacing. The diameter of the holes was reduced to 180 nm for all the samples, to allow for fabricating arrays with a periodicity of 400 nm. The center-to-center hole spacing was selected to be 175 nm in order to produce sharp apexes and the array periodicity was varied from 380 nm to 750 nm. The short periodicities were chosen to be resonant with the second harmonic wavelength, which is around 400 nm, where new resonance phenomena are possible.

Figure 5 shows the linear transmission measurements for the second set of samples. For simplicity, only four periodicities are shown: 430 nm, 580 nm, 690 nm, and 750 nm. The measurements have been normalized to the spectrum of the incident beam. The surface area of each array was kept constant and so the number of holes decreased by the square of the array periodicity. The baseline offset between the different spectra is attributed to direct transmission through an increased number of holes in arrays with shorter periodicity. For example, there are 2.8 times more double holes at the 430 nm periodicity than at 750 nm.

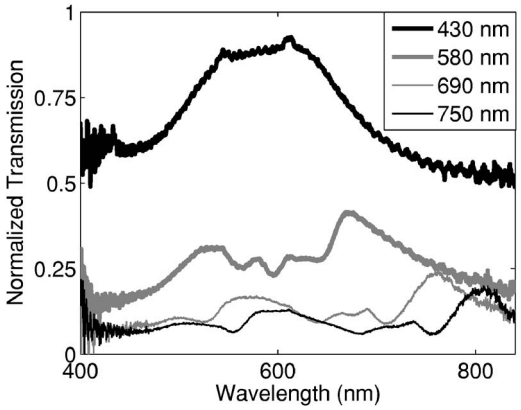

FIG. 5. Linear transmission spectra for different periodicities, l, (430, 490, 580, and 750 nm).

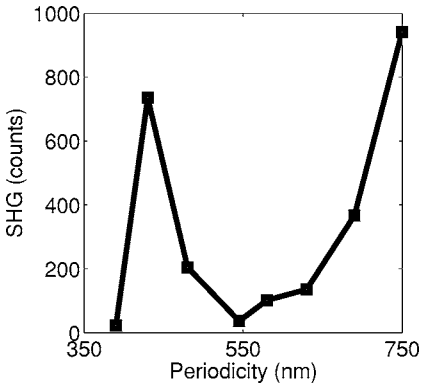

FIG. 6. Periodicity dependence of SHG for a 10° angle of incidence.

For the 580 nm periodicity, the (1,0) and the (1,1) resonances are situated at the wavelengths of 670 nm and 530 nm. For $l=430$ nm, there is a 140 nm wide resonance. For the other periodicities between 545 nm and 750 nm, the trend is the same. For smaller periodicities, there is only one broad maximum that arises from a double peak.[24]

Figure 6 shows the SHG measurements performed with an angle of incidence of 10° for different periodicities. The SHG is largest for the 750 nm periodicity, which is due to the (1,0) resonance at 800 nm, as can be seen in Fig. 5. That resonance is at the same central wavelength of the Ti:Sapphire laser. For smaller periodicities, the (1,0) resonance moved to the shorter wavelength so that the SHG signal decreased. The enhancement of the fundamental beam by the array periodicity leads to an increased SHG signal.

Figure 7 shows the angle-dependent SHG measurements for $l=430$ nm and $l=750$ nm. The 750 nm periodicity has a maximum for a 8° angle of incidence while the 480 nm periodicity has a maximum for a 12° angle of incidence. The signal is small for angles less than 5° and for angles greater than 15°. The maximum SHG for these two different periodicities has a similar number of counts but for different angles of incidence. A further discussion of these results is given in the next section.

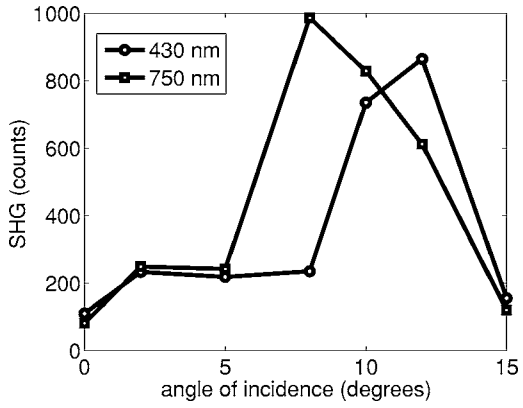

FIG. 7. Angle-dependent SHG measurements for two arrays: $l=430$ nm and $l=750$ nm.

IV. DISCUSSION

A. Field-enhancement with double-hole centre-to-centre spacing

Some of the features of the angle-dependent SHG measurements are similar to SHG on circular and triangular hole shapes.[19] In that work, the circular-holes did not allow SHG for angle of incidence smaller than 20° while triangular holes allowed SHG for a 8° angle of incidence. There are, however, notable differences for the double-hole structure. By varying the center-to-center hole spacing with fixed array periodicity, we found that the circular hole arrays had a maximum SHG signal for a 12° incidence angle while the double-hole array has a maximum SHG for smaller incidence angles with a maximum at 8°.

It was shown previously that noncentrosymmetric holes provide increased SHG for reduced angles of incidence with respect to centrosymmetric holes.[19] The double-hole still has inversion symmetry about the angle of incidence, so this is not expected to be the dominant contribution to observing SHG at smaller angles. There is a second parameter which influences the SHG angle dependence: the main peak of the Bragg resonance is redshifted by changing the angle of incidence.[8] This influences the resonant enhancement of both the fundamental beam and the SHG. Therefore, by changing the angle of incidence, the maximum local field enhancement can be varied and correspondingly, the SHG is enhanced. The sample was rotated along the x axis. Due to the small angle of rotation, this modifies the Bragg conditions for the lattice only slightly, but has a large effect on breaking the symmetry of the system, and thereby increasing the SHG, as shown in Fig. 4. For these small angles of rotation, the polarization dependence of the incident beam and the second harmonic are not modified significantly.

For nonlinear spectroscopy applications, the most important aspect of the double-hole structure is the enhanced local field at the apexes. Because the maximum SHG varies with incidence angle as the center-to-center hole spacing is varied, a comparison was made for the maximum SHG over all angles of incidence: a 14 times enhancement was found between the maximum for the array with $d=0$ nm (single circular holes) and $d=195$ nm (double holes with sharp apexes). This significant ratio is from the local enhancement of the electric field at the apexes. By comparison, triangular holes gave only a 1.7 enhancement factor when compared with circular holes.[19] In spite of the presence of sharp edges in the triangular shape, the SHG enhancement was not significant, while the double-hole with apexes presented here gives a large SHG enhancement.

Although the SHG is enhanced by a factor of 14, the local field is expected to be enhanced by a significantly greater value since the SHG is mainly from an extremely localized area around the apexes. We have performed FDTD simulations of double-hole structures to investigate how the proximity and sharpness of the apexes influence the local electric field intensity.[22] In that work, the maximum local electric field calculated was four orders of magnitude higher for the double-hole structure with apexes than for a double-hole

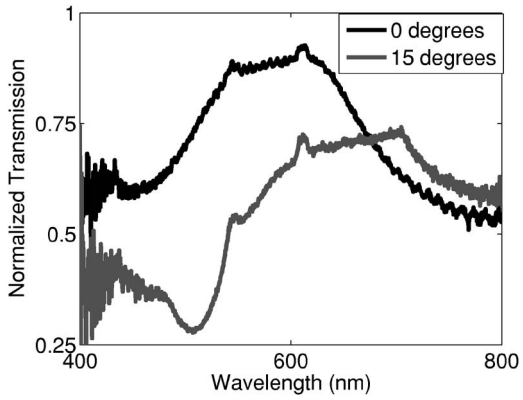

FIG. 8. Linear transmission measurements for $l=430$ nm with two angles of incidence: 0° and 15°. The measurements are normalized by the incident beam.

structure without apexes. Therefore, the enhancement of the SHG arises from a localized region about the apexes.

B. Fundamental and second-harmonic resonances with array periodicity

By changing the periodicity of the arrays of double-holes, two separate contributions to the enhanced SHG are observed. The first is from resonance with the fundamental wavelength and the second is from resonance with the second-harmonic wavelength. The contribution of the fundamental wavelength is seen clearly when the periodicity is varied to shorter wavelengths than 750 nm. As the periodicity decreases from 750 nm to 690 nm, Fig. 5 shows that the linear transmission (1,0) resonance peak decreases from 800 nm to 760 nm. The fundamental wavelength (pulse source center) is at 800 nm, so a strong SHG signal is observed for the 750 nm periodicity. The linear transmission is reduced by a factor of 1.8 (removing the baseline offset) at the wavelength of 800 nm when the periodicity is reduced to 690 nm. Correspondingly, the SHG is reduced by a factor 3 as the periodicity is shifted out of resonance with the fundamental beam. This is nearly a square dependence that is expected from SHG; however, the linear transmission is not a measurement of the local field at the surface of the gold that produces the SHG, so this comparison should not be taken to imply a direct correspondence between the two measurements.

The SHG is also maximized for a shorter periodicity of 430 nm, as seen in Fig. 6. This is very close to the second harmonic wavelength of 400 nm. In addition, the linear transmission spectra show a maximum near 400 nm for that periodicity; however, the measurement has much lower sensitivity at that wavelength because of the halogen light source and the spectrometer. The linear transmission spectrum was also taken for an angle of 15° for all the samples. Figure 8 shows the variation of the linear transmission spectrum for two angles for the 430 nm periodicity. There is a more pronounced peak at the shorter wavelengths for the angled sample; however, the overall transmission is reduced as a result of tilting the sample.

It has been shown that an enhanced linear response at the second harmonic wavelength will result in an enhanced nonlinear response too.[25] This has been formulated approximately as

$$R = |L(2\omega)L(\omega)^2|,$$

where R is the enhancement, $L(2\omega)$ is the linear response at the SHG wavelength and $L(\omega)$ is the linear response at the fundamental wavelength. This is consistent with the enhanced response seen here for arrays of double-holes when the $L(2\omega)$ increases, as shown in Fig. 6.

The fundamental and second-harmonic resonant enhancements to the SHG are both angle dependent, as shown in Fig. 7. For small angles, there is nearly no SHG signal since the centrosymmetry of the sample was not broken sufficiently. The maximum SHG was measured for an 8° angle for the 750 nm periodicity. For the periodicity of 430 nm, SHG signal was measured only for angles greater than 8°. This is attributed to the momentum matching condition between the second harmonic and the resonance wavelength that is obtained by tilting the angle of incidence, as shown on Figure 8. As an aside, for $l=750$ nm, the SHG angle-dependent measurements were the same as the first set of samples, which demonstrates good reproducibility of the results for different fabrications runs.

V. CONCLUSIONS

Apex-enhanced SHG from arrays of double-holes in a gold film was studied. The double holes are readily fabricated by varying the distance between two single holes to produce sharp apexes when the holes overlap. A 14 times enhancement factor in the SHG was measured, as compared to circular holes. The strong angular dependence of the SHG was attributed to the effects of momentum matching to the Bragg resonances of the array and symmetry breaking to create an SHG signal. The periodicity of the array also has a strong influence on the SHG, and this dependence follows the peaks in the linear transmission. Two different resonance phenomena are observed when tuning the array periodicity: resonance with the fundamental beam or with the second harmonic beam. The linear transmission (1,0) Bragg resonance was tuned by varying the periodicity. While the fundamental beam is resonant for the periodicity of 750 nm, the second harmonic is resonant for the periodicity of 430 nm, and increased SHG is observed for both these periodicities. Between these periodicities, the SHG is reduced. The angle-dependent SHG and linear transmission measurements also supports this correlation.

From these measurements, it is clear that the double-hole structure is a good candidate for applications that require strong electric field focusing at the nanoscale. Here we have shown that the application may be optimized by changing the center-to-center hole spacing, the array periodicity and the angle of incidence to match the wavelengths of interest. For example, SERS measurements in the optical range should be from the double-hole structure by tuning the resonances to the excitation and scattered wavelengths.

[1] S. I. Bozhevolnyi, J. Beermann, and V. Coello, Phys. Rev. Lett. **90**, 197403 (2003).
[2] A. G. Brolo, E. Arctander, R. Gordon, B. Leathem, and K. L. Kavanagh, Nano Lett. **4**, 2015 (2004).
[3] P. Muhlschlegel, H. J. Eisler, O. J. F. Martin, B. Hecht, and D. W. Pohl, Science **308**, 1607 (2005).
[4] M. I. Stockman, Phys. Rev. Lett. **93**, 137404 (2004).
[5] K. Li, M. I. Stockman, and D. J. Bergman, Phys. Rev. Lett. **91**, 227402 (2003).
[6] P. J. Schuck, D. P. Fromm, A. Sundaramurthy, G. S. Kino, and W. E. Moerner, Phys. Rev. Lett. **94**, 017402 (2005).
[7] P. Mühlschlegel, H. J. Eisler, O. J. F. Martin, B. Hecht, and D. W. Pohl, Science **308**, 1607 (2005).
[8] T. W. Ebbesen, H. J. Lezec, H. F. Ghaemi, T. Thio, and P. A. Wolff, Nature (London) **391**, 667 (1998).
[9] R. Gordon, A. G. Brolo, A. McKinnon, A. Rajora, B. Leathem, and K. L. Kavanagh, Phys. Rev. Lett. **92**, 037401 (2004).
[10] K. J. Klein Koerkamp, S. Enoch, F. B. Segerink, N. F. Van Hulst, and L. Kuipers, Phys. Rev. Lett. **92**, 183901 (2004).
[11] K. L. Van Der Molen, K. J. Klein Koerkamp, S. Enoch, F. B. Segerink, N. F. Van Hulst, and L. Kuipers, Phys. Rev. B **72**, 045421 (2005).
[12] A. Degiron, H. J. Lezec, N. Yamamoto, and T. W. Ebbesen, Opt. Commun. **239**, 61 (2004).
[13] R. Gordon and A. G. Brolo, Opt. Express **13**, 1933 (2005).
[14] R. Gordon, M. Hughes, B. Leathem, K. L. Kavanagh, and A. G. Brolo, Nano Lett. **5**, 1243 (2005).
[15] K. H. Benneman, in *Nonlinear Optics in Metals* (Clarendon, Oxford, 1998).
[16] A. V. Zayats, T. Kalkbrenner, V. Sandoghdar, and J. Mlynek, Phys. Rev. B **61**, 4545 (2000).
[17] C. C. Neacsu, G. A. Reider, and M. B. Raschke, Phys. Rev. B **71**, 201402(R) (2005).
[18] N. Rakov, F. E. Ramos, and M. Xiao, J. Phys. Condens. Matter **15**, L349 (2003).
[19] M. Airola, Y. Liu, and S. Blair, J. Opt. A, Pure Appl. Opt. **7**, S118 (2005).
[20] A. Nahata, R. A. Linke, T. Ishi, and K. Ohashi, Opt. Lett. **28**, 423 (2003).
[21] A. Lesuffleur, L. K. S. Kumar, and R. Gordon, Appl. Phys. Lett. **88**, 261104 (2006).
[22] L. K. S. Kumar, A. Lesuffleur, M. Hughes, and R. Gordon, Appl. Phys. B **84**, 25 (2006).
[23] T. Atay, J.-H. Song, and A. V. Nurmikko, Nano Lett. **4**, 1627 (2004).
[24] A. Degiron and T. W. Ebbesen, J. Opt. A, Pure Appl. Opt. **7**, S90 (2005).
[25] M. L. Sandrock, C. D. Pibel, F. M. Geiger, and C. A. Foss Jr., J. Phys. Chem. **130**, 2668 (1999).